Int J Thermophys (2008) 29:735–749
DOI 10.1007/s10765-007-0361-1

Influence of Water on the Total Heat Transfer in 'Evacuated' Insulations

Ulrich Heinemann

Published online: 5 February 2008

Abstract The impact of water vapor on the thermal conductivity of vacuum insulation panels (VIPs) filled with fumed silica kernels was investigated and found to be surprisingly large. Besides thermal transport by water vapor within the pore space, the question was whether water in the adsorbed phase also contributed significantly to the total heat transfer. In order to quantify these effects, several series of thermal conductivity measurements were performed in an evacuable guarded-hot-plate. The fumed silica specimens were first investigated in the dry state. Then water vapor was added into the vacuum system in different quantities (valves closed and no pumping), yielding water content in the VIP-kernel of up to 4% by mass. Most of the water is adsorbed in the specimens; smaller amounts are to be found in the gas phase. The parameter varied was the temperature; accordingly, the partial pressure of water vapor changed. An empirical equation is presented that describes the influence of water vapor and adsorbed water on the total heat transfer.

Keywords Coupled heat transfer · Guarded hot plate · Moisture · Thermal conductivity · Thermal insulation · Vacuum insulation panels

1 Introduction

Different kinds of filler materials, such as glass–fiberboards, pressed powder boards, or special open porous and, thus, evacuable foams are used as core material for vacuum insulation panels (VIPs) [1]. The minimum requirements to the quality of the vacuum, that has to be achieved and maintained, are found for nanostructured materials.

U. Heinemann (✉)
Bavarian Center for Applied Energy Research e.V. (ZAE Bayern), Am Hubland,
97074 Wuerzburg, Germany
e-mail: ulrich.heinemann@zae.uni-wuerzburg.de

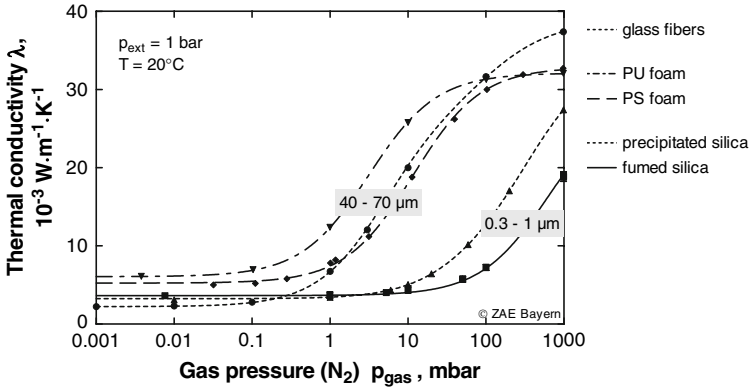

Fig. 1 Thermal conductivity of different filler materials more or less optimized for the application in VIPs. External pressure is 1 bar; the temperature is 20°C

For example, in boards made of pressed fumed silica even at an internal gas pressure of 2,000 Pa the contribution of the gas to the total heat transfer is nearly eliminated (see Fig. 1) [2]. For these extremely fine-structured core materials, the requirements for the tightness of the envelope are relatively moderate and thus special high barrier metalized laminates consisting mainly of polymers and extremely thin Al-layers can be used for the envelope. As for all plastic films and for these high-grade films, the transmission rate for water vapor is several orders of magnitude larger than those for oxygen or nitrogen [3]. Thus, the impact of water on the thermal conductivity was investigated. It was found to be larger than expected for the gaseous conductivity of water vapor within the pore space. We pursued the question of whether or not also water in the adsorbed phase contributes to the total heat transfer. In order to quantify these effects, several series of thermal-conductivity measurements were performed in an evacuable guarded-hot-plate [4]. The aim of the investigations was to formulate an empirical equation that describes the influence of water vapor and adsorbed water on the total heat transfer.

The fumed silica specimens were first investigated in the dry state. Then water vapor was added into the vacuum system in different quantities (valves closed and no pumping), yielding water content in the VIP-kernel of up to 4% by mass. Most of the water is adsorbed in the specimen; smaller amounts are found in the gas phase. The parameter varied was the mean temperature and, thus, accordingly the partial pressure of water vapor.

2 Thermal Transport in Porous Insulations

2.1 Heat Transfer in Dry Insulation Materials

In highly porous insulation materials such as foams, fiber-boards, or pressed powder boards, the total heat transfer occurs via conduction along the solid structure, conduction of the gas within the hollow spaces, and infrared radiative transfer. Convection, a very efficient heat transfer mechanism, usually is suppressed in insulation materials

used at ambient conditions with moderate temperature gradients. In a simple approach, the total thermal conductivity λ could be described as the sum of the gaseous conductivity λ_{gas}, the solid conductivity λ_{sc} and the radiative conductivity λ_{rad}. As this simple approach implies individual temperature characteristics for each heat transfer path, local coupling of the different mechanisms results in a more or less enhanced total conductivity. These effects may be accounted for with an additional coupling term λ_{coupl} [5]:

$$\lambda = \lambda_{gas} + \lambda_{sc} + \lambda_{rad} + \lambda_{coupl}. \tag{1}$$

Significant coupling effects have been observed in semi-transparent media like monolithic aerogels or low-density foams in combination with low-emissivity boundaries or integrated radiation shields [6,7], as well as in materials with dot-like contacts between fibers and grains [8]. For example, in a bed of glass spheres, comparing the total thermal conductivity of the evacuated and the non-evacuated specimen, the contribution from the gas is seven times as large as expected just from the thermal conductivity of still air [4]. In both cases for a single heat transfer mechanism, there are localized steep temperature gradients which are related to high thermal resistances. These thermal resistances may be shorted out by other mechanisms.

In optically thick foams with a non-broken structure, coupling effects may be neglected. In the evacuated case in optically thick media, the total conductivity λ_{evac} is

$$\lambda_{evac} = \lambda_{sc} + \lambda_{rad}. \tag{2}$$

The variation of the gaseous conductivity with gas pressure p depends on the size of the (largest) pores:

$$\lambda_{gas} = \lambda_{gas,0}/(1 + 2\beta \cdot Kn) = \lambda_{gas,0}/\big(1 + p_{1/2}/p\big), \tag{3}$$

where $Kn = l/\Phi$ the Knudsen number, l is the mean free path of the gas molecules, and Φ is the pore width. $\lambda_{gas,0}$ is the thermal conductivity of the free still gas, and ß is a constant which, in addition to other factors, is determined by the accommodation coefficient α [8]. α describes the efficiency of energy transfer when gas molecules hit the solid structure. It depends on temperature and on the collision partners. For air at 300 K, $\lambda_{gas,0} = 0.026\,\mathrm{W \cdot m^{-1} \cdot K^{-1}}$, and ß ≈ 1.5. $p_{1/2}$ is the gas pressure at which the gaseous thermal conductivity is equal to $\lambda_{gas,0}/2$. For a given temperature and gas, it is a characteristic property of the insulation material. It may be derived from thermal-conductivity measurements as depicted in Fig. 1.

Looking at the temperature dependence of the total thermal conductivity, temperature dependencies of all contributions have to be considered: the radiative contribution varies with the third power of absolute temperature, if the extinction coefficient is temperature independent. For amorphous materials at ambient conditions, the temperature dependence of the solid conduction can be considered to be the same as for the bulk material. For the gaseous contribution for ideal gases, $\lambda_{gas,o} \propto \sqrt{T}$ and $l \propto T$. More precise considerations also take into account spectral variation of the infrared properties and variations in the accommodation coefficient.

Considering the influence of other gases on the total heat transfer, modified parameters for the thermal conductivity of the still free gas $\lambda_{gas,0}$, another mean free path l, and another constant ß, and possibly also another accommodation coefficient α, have to be taken into account.

2.2 Heat Transfer in Moist Porous Materials

The modeling of the coupled heat and moisture transport in porous materials is a major research topic, especially in building physics. In contrast to heat conduction, there is no universal theory for the driving forces and transport parameters in the case of moisture transport [9]. Besides influences on the parameters describing the heat transfer of the dry material, i.e., such as a reduced infrared radiative transfer, an increased 'solid' conduction by the (non-moving) liquid film, especially when moisture is adsorbed at thermally sensitive dot-like contacts, and a modified gaseous contribution (see above), the diffusion of vapor in the gaseous phase and of water along the surface have to be considered. Also, in the hygro-thermal steady state which may be achieved in encapsulated insulating materials (as in VIPs) where there is no net moisture transport through the panel, significant or even dominant additional contributions to the total heat transfer may arise from permanent de- and adsorption of water in the hot and cold regions, respectively, of the specimen and counterbalanced flow in the liquid and gaseous phases. Due to large amounts of latent heat from phase changes, this so-called heat-pipe effect is a very efficient heat transfer mechanism, and thus should be avoided in thermal insulations.

2.3 Measurement Method

Thermal-conductivity experiments on moist materials are complicated by the additional transport processes of water de- and adsorption and vapor, surface, and capillary diffusion. Suitable for the measurement of moisture effects on heat transfer are long-term measurements with a guarded hot-plate or a heat flow-meter apparatus (see, e.g., [10]), such that stationary conditions are guaranteed.

Such thermal-conductivity measurements, in principle, require a temperature gradient, which causes a moisture redistribution in the material. When thermal and moisture equilibrium are reached, moisture transfer by vapor diffusion is counterbalanced by moisture back-transfer along the solid surfaces.

Depending on the water content and on the adsorption characteristics of the material, nonlinear moisture profiles also have to be taken into account. Thus, one has to consider that the measured thermal conductivity is an apparent one.

3 Investigations on 'Evacuated' Fumed Silica

3.1 Investigated Material

Boards made by compression of fumed silica powder, mixed with organic fibers for reinforcement and some infrared opacifier, proved to be a good filler material for VIPs [2]. The subject of the investigations described here were such boards, produced by

the company Wacker Chemie GmbH/Kempten, Germany, labeled by WDS-NT. The density of the material, loaded with an external pressure of 1 bar, was $170\,\mathrm{kg{\cdot}m^{-3}}$.

Two sets of measurements were performed over a period of approximately 18 months. In the meantime, the samples were stored in the lab.

Measurements of the thermal conductivity on the same type of material, performed on the preheated, dry material, were reported, e.g., in [2]. The first investigations on the influence of water on the thermal conductivity on specially prepared VIPs are described in [11].

3.2 Sorption Characteristic

The sorption isotherm was measured by the company Quantachrom/Odelzhausen, Germany on the Wacker WDS-VIP material based on fumed silica of the type T30 with a specific surface area of about $300\,\mathrm{m^2{\cdot}g^{-1}}$. It is assumed that there is no significant difference in the sorption behavior for the materials labeled WDS-NT and WDS-VIP. Initially the material was dried under vacuum for 3 h at 150°C. The sorption isotherm then was determined for an adsorption cycle and subsequently a desorption cycle at a temperature of 23°C.

As the material investigated is meso/macroporous, no micro-pore condensation is observed. Thus, water content by mass X_w and relative humidity φ in the low humidity region correlate almost linearly,

$$X_\mathrm{w} = 0.08\, m\%\varphi/\%. \tag{4}$$

This holds up to $\varphi = 60\%$. For a higher humidity, polynomial approximations may be used. From the inverse function $\varphi(X_\mathrm{w})$ of the sorption isotherm $X_\mathrm{w}(\varphi)$, one can determine the water vapor pressure p_wv for a given water content in the material. As the saturated vapor pressure increases exponentially with temperature, one gets

$$p_\mathrm{wv} = \varphi(X_\mathrm{w})\, p_\mathrm{wv.saturated}(T). \tag{5}$$

The adsorption isotherm is assumed to be almost independent of temperature.

3.3 Modeling of the Moisture Distribution in Samples with Temperature Gradient

In a zero-order approximation it was assumed that for a thermal and hygric steady state there is no vapor or surface diffusion. From these conditions a constant water vapor partial pressure results for the material. According to Eq. 4, the relative humidity in the specimen varies with the reciprocal of the saturated vapor pressure. Consequently, a nonlinear moisture distribution is expected.

Numerical calculations were performed with the following input parameters: the total water content in the VIP, the mean temperature, and the temperature gradient. In addition to material data, the mean of de- and ad-sorption isotherms, approximated as depicted in Fig. 2 was used, emulating the situation of a VIP that has been dried in the production process and in which water vapor has penetrated though the envelope.

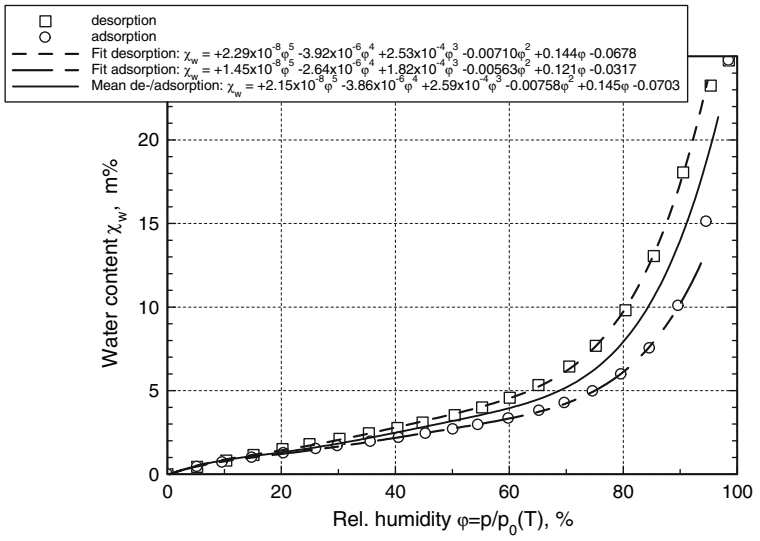

Fig. 2 Sorption isotherm for Wacker WDS-VIP derived at 23°C. Measured data for the adsorption and desorption cycles are depicted together with fit equations used for numerical calculations (see text). Measurements by Quantachrom

A typical situation of interest in practical application of VIPs in buildings is depicted in Fig. 3. The total water content of 3% in mass corresponds to a mean humidity of about 45%. This is a humidity close to the mean annual humidity in a building façade. Two effects may become obvious from this figure:

- The non-linearity is especially pronounced when the relative humidity exceeds the linear region of the adsorption isotherm. This is the case when the temperature spread is increased to $\Delta T = 20\,\mathrm{K}$.
- The water vapor partial pressure varies with the temperature gradient. As a consequence, the influence of the vapor on the total heat transfer is also expected to vary with the temperature gradient. Thus, again, in principle, an apparent thermal conductivity will be derived from the experiments.

In Fig. 4 the analogous situation, but for a mean temperature of 50°C, is depicted. For the same temperature gradient the moisture concentration on the cold side is less pronounced at the higher temperature level.

From Fig. 5 it becomes obvious that for an increasing water content most of the water is adsorbed on the cold side of the panel, if the relative humidity at the cold side exceeds the linear region of the adsorption isotherm. In this figure the adsorption isotherm was used. The approximation that no moisture back transfer along the solid backbone occurs is not realistic—except for temperatures below 0°C, when the mobility of the water network is strongly reduced. In reality, the moisture accumulation on the cold side is reduced by this back transfer and, thus, the moisture distribution shown in Figs. 3 and 4 will be depressed.

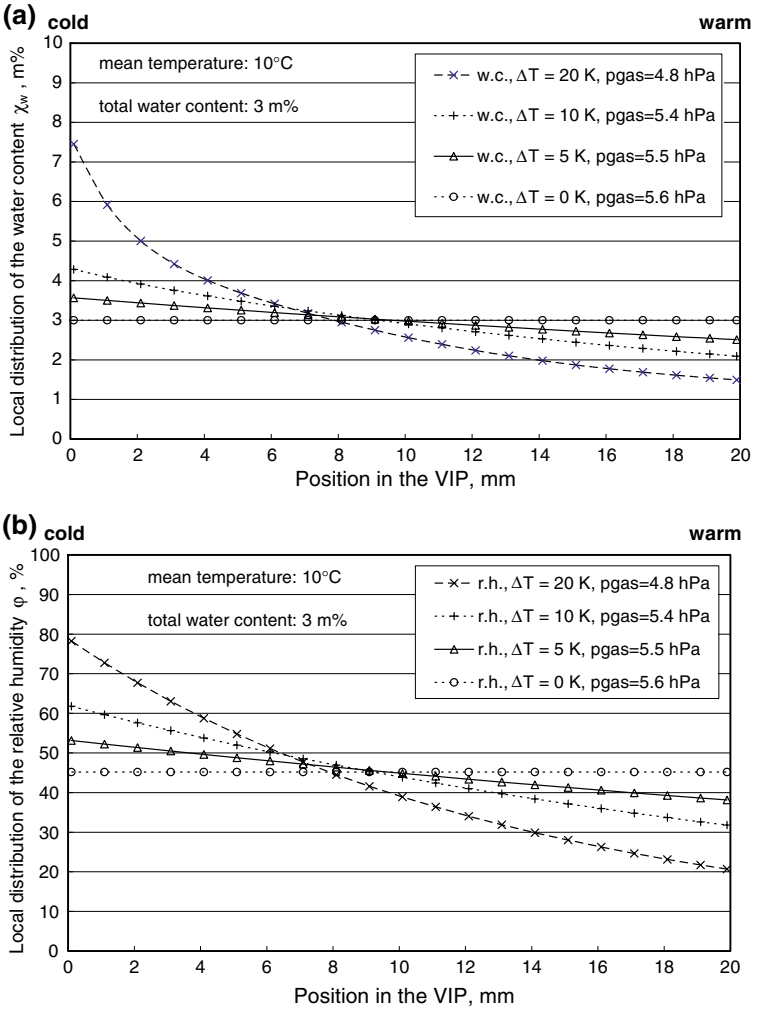

Fig. 3 (**a**) Moisture distribution and (**b**) related relative humidity in a VIP with a thickness of 20 mm, for a total water content of 3% in mass. For the same mean temperature of 10°C, the temperature spread ΔT was varied. Average relative humidity is about 45%

3.4 Thermal Conductivity Measurements with an Evacuable Guarded-Hot-Plate Apparatus

3.4.1 Experimental Setup

Two series of thermal-conductivity measurements were performed with the ZAE-constructed evacuable, pressure-loadable guarded-hot-plate apparatus LOLA 4 (Fig. 6).

The apparatus was modified in two ways. First, the electrically controlled cold plates were removed. The temperature on the cold sides then was directly controlled

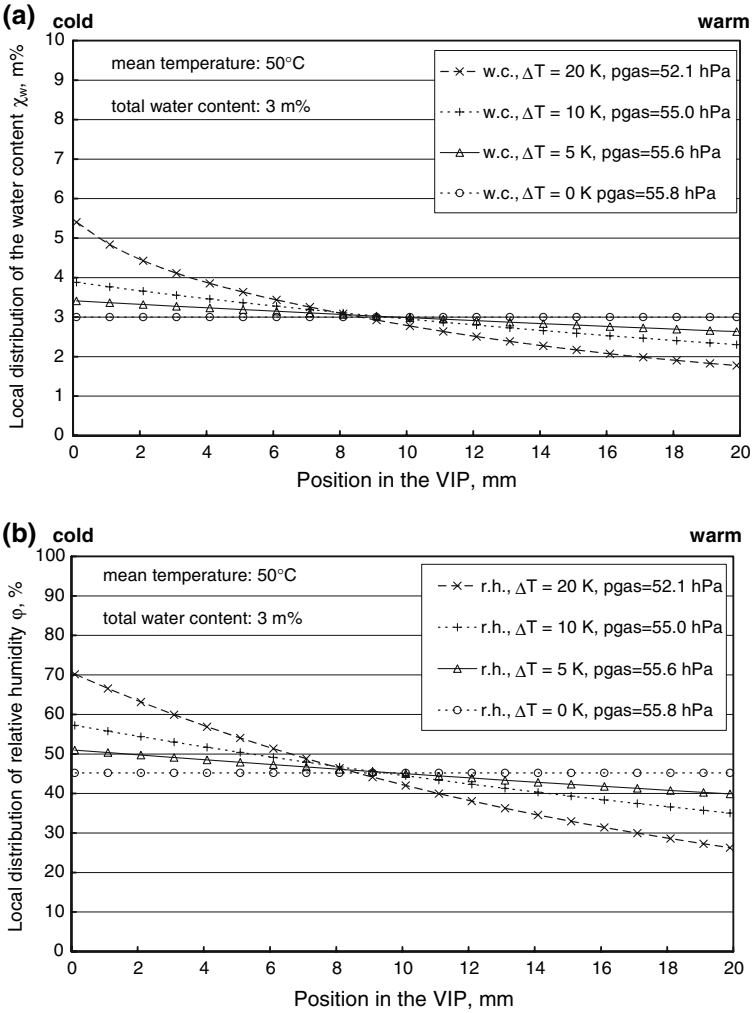

Fig. 4 (**a**) Moisture distribution and (**b**) related relative humidity as in Fig. 3. Mean temperature here is 50°C

by an external fluid thermostat. The maximal achievable water vapor pressure in the apparatus is limited by the temperature of the coldest parts in the apparatus. These are either the heat sinks—for measurements at temperatures below room temperature—or the outer walls of the vacuum chamber for measurements at elevated temperatures.

Secondly, a source of water vapor as shown in Fig. 7 was flanged to the apparatus. It consists of a small chamber partially filled with water. Via a first valve, it can be evacuated to the water vapor pressure. Via a second valve, water vapor can be fed into the apparatus.

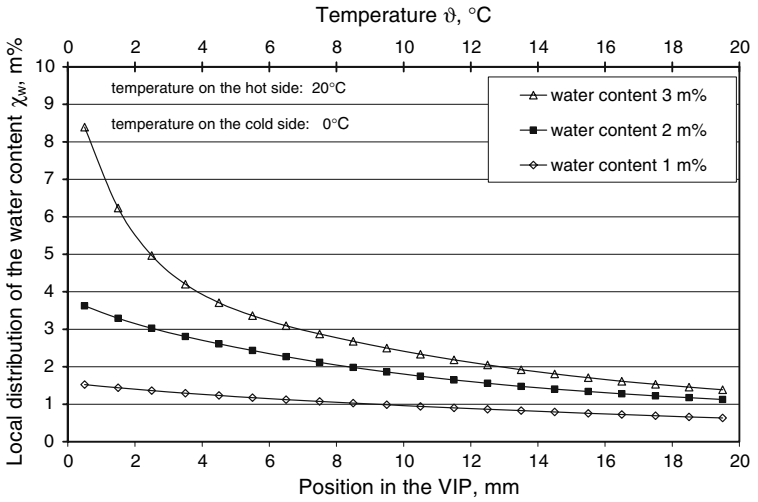

Fig. 5 Moisture distribution in a VIP with a thickness of 20 mm, temperature on the hot side 20°C and on the cold side 0°C. The total water content was varied

Specifications:

Measurable variable thermal conductivity:
0.0001 to 0.1 $W \cdot m^{-1} \cdot K^{-1}$

temperature range:	-200 °C to 400 °C
internal gas pressure: (different gases)	10^{-5} mbar to 1000 mbar
external load pressure:	0 to 1.5 bar
emissivity of the surfaces:	0.8 to 0.04

samples (two identical):

thickness:	1 to 28 mm
diameter:	280 mm

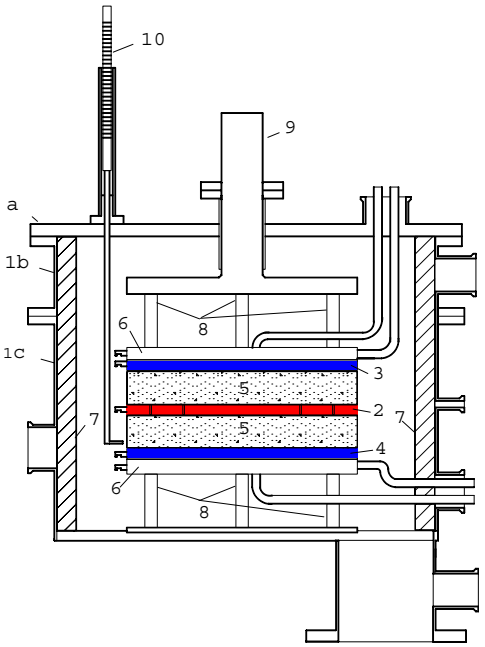

Fig. 6 Diagram of the two-plate apparatus LOLA 4: 1. vacuum chamber, 2. hotplate with two guard rings, 3, 4. cold plates, 5. samples, 6. heat sinks, 7. insulation, 8. ceramic supports, 9. vacuum-tight guided stamp, 10. three thickness sensors

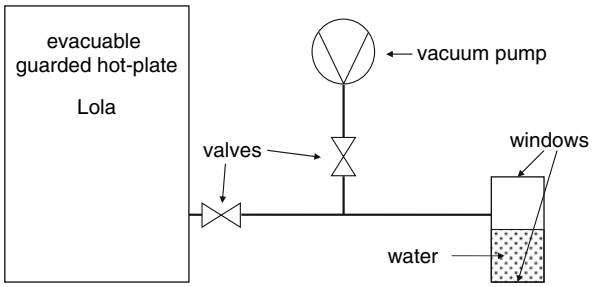

Fig. 7 Diagram of the source for water vapor (not drawn to scale)

If in 'evacuated' moist vacuum insulations the water vapor partial pressure reflects the total pressure from the measured pressure and the mean temperature of the samples, the amount of water adsorbed by the samples can be calculated.

In order to check that stationary conditions had been achieved in the thermal-conductivity measurements, measurements were repeated at the same temperature gradient across the specimen of 20 K, on the hand with a smaller gradient, and on the other hand, with an applied larger temperature gradient. Thus, effects of the water-vapor redistribution come from the opposite side. For example, we started off with a relatively small temperature gradient of 10 K across the specimens, then increased the temperature difference to 20 K and measured the apparent thermal conductivity. Afterwards, a larger temperature difference (about 30 K) was applied to achieve a more pronounced distribution of water. Then the thermal conductivity measurement was repeated for 20 K. As we got consistent thermal conductivity values in both cases, we took this as proof for thermal transport and moisture distribution. Typical duration to obtain one data point ranges from about 4 h for the dry specimens up to several days for the specimens with additional humidity.

From the variation of the temperature, the temperature gradient and the water content, data for practical applications can be gained; secondly, these data should be the basis for an empirical description of the influence of water on the heat transfer in 'evacuated' fumed silica insulations.

3.4.2 Measurement Results

Initially the temperature and gas pressure dependencies of the thermal conductivity were determined for the dry samples (Fig. 8).

Within the temperature range investigated the different nonlinearities in the temperature dependences of the solid conductivity and the radiative conductivity obviously compensate each other. The temperature dependence of the evacuated specimen thus can be described by a linear function:

$$\lambda_{\mathrm{evac}} \,/\, 10^{-3}\ \mathrm{W \cdot m^{-1} \cdot K^{-1}} = 0.0124T/\mathrm{K} + 0.808 \tag{6}$$

From the gas pressure dependence a characteristic pressure $p_{1/2} = 715$ hPa is derived when performing a fit for the total range up to 1 bar. A somewhat smaller value of

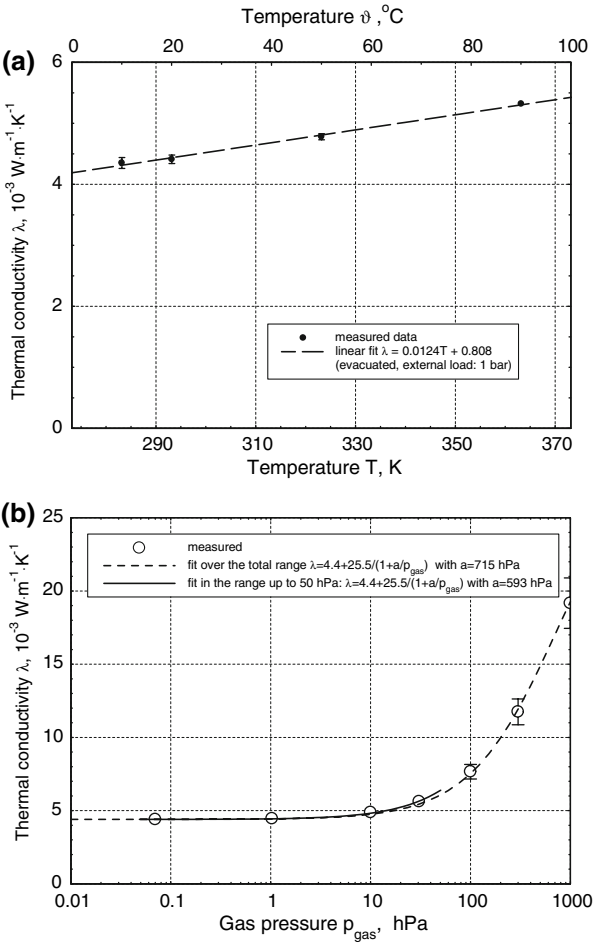

Fig. 8 Thermal conductivity of the dry material versus (**a**) the temperature (evacuated, left figure) and versus (**b**) the N_2-gas pressure (mean temperature 20°C). For all measurements the external load on the samples was 1 bar

about 600 hPa is found when applying a fit only up to 50 hPa, the range where the influence of water vapor pressure will be studied in detail.

In Fig. 9 the results of several sets with different amounts of water in the apparatus are depicted. From Fig. 9a linear dependences of the conductivity on the water content seem to hold for all temperatures investigated. As one might expect from the increase of water vapor pressure with temperature for a fixed humidity (vertical line), the effect of moisture also increases with temperature, resulting in an increased slope in this figure for higher temperatures.

The Fig. 9b resembles conditions close to the situation in building applications (mean temperature of 20°C). The measured thermal conductivity is depicted for different water content versus the corresponding H_2O-gas pressure and the N_2-gas.

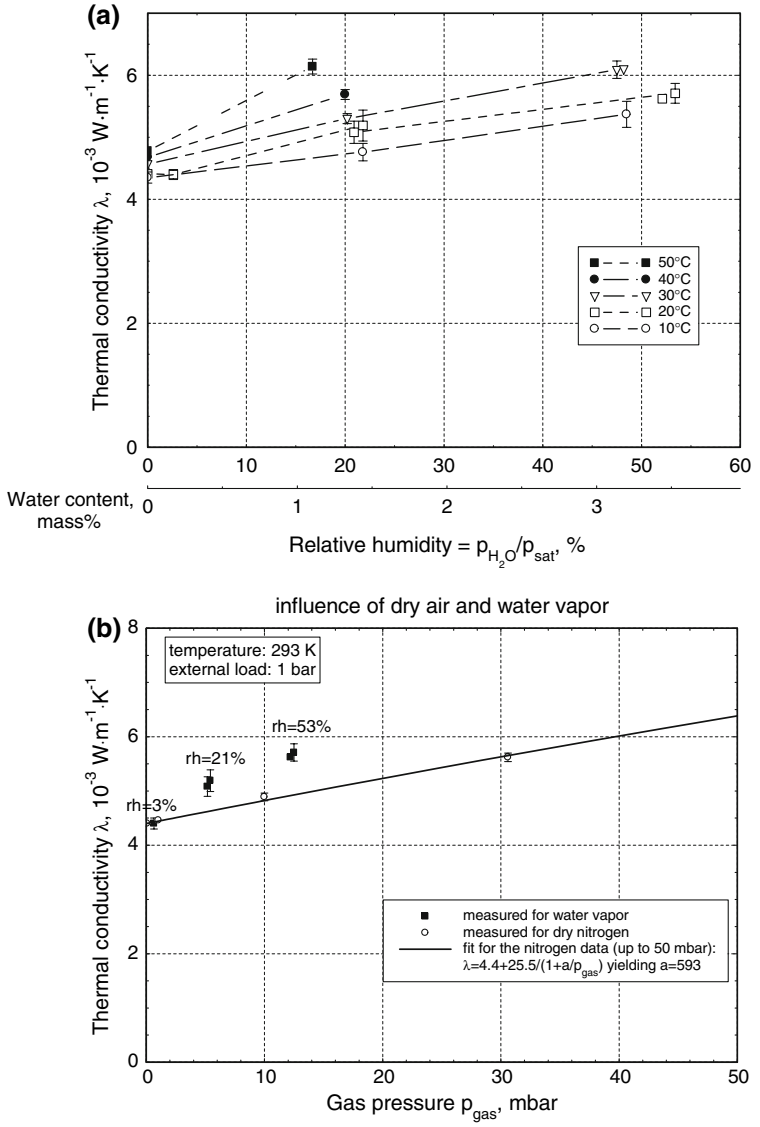

Fig. 9 (**a**) Measured thermal conductivity as a function of different relative humidities for different mean temperatures and (**b**) values obtained for 20°C for different H_2O and N_2-gas pressures. Temperature spread was 20 K

Both variations may be interpreted as the maximum degradation effects for VIPs employed in buildings: the onset in the thermal conductivity by penetrating air (assuming a pressure increase by air of 1 mbar per year), and in the extreme case, an equilibrium of internal and mean annual humidity outside a VIP.

The second series of measurements was thought to improve the data basis for theoretical considerations, especially to check whether the thermal conductivity increases caused by air and by moisture may be simply added.

Even though the relationship of the total heat transfer and moisture content, temperature, and temperature gradient may be very complex, a simple approach was tested to describe the total thermal conductivity as a function of humidity and temperature.

Some assumptions and approximations were as follows:

- At first only measured data have been selected where the temperature spread was 20 K.
- The temperature dependence of the thermal conductivity of the evacuated, dry specimen was assumed to be linear, as found above.
- For the low gas pressure range considered here, the Knudsen formula was approximated as:

$$\lambda_{\mathrm{gas}} = \lambda_{\mathrm{gas},0}/(1 + p_{1/2}/p) \approx \lambda_{\mathrm{gas},0}/p_{1/2}/p = \frac{\lambda_{\mathrm{gas},0}}{p_{1/2}} p, \tag{7}$$

- As temperature effects of the thermal conductivity of free, still gas $\lambda_{\mathrm{gas,o}} \propto \sqrt{T}$ and that of the mean free path $l \propto T$ are opposed, the resulting effect is expected to be small for the small temperature range considered here. Thus, no temperature dependence was assumed for the ratio $\lambda_{\mathrm{gas,o}}/p_{1/2}$.
- For adoption of the different kind of gases (H_2O and N_2) in the Knudsen formula for the same reason, a constant factor was used.

The most influencing variables are assumed to be:

- adsorbed water in the 'liquid' phase, which is assumed to increase the 'solid' conduction proportional to the amount of adsorbed water; and
- in the gaseous phase by the partial water vapor pressure $p_{\mathrm{H_2O}}(T) = \varphi p_{\mathrm{sat}}(T)$ with $p_{\mathrm{sat}}(T)/\mathrm{hPa} = 6.11 \exp\left(17.08 \frac{T/\mathrm{K}-273.15}{T/\mathrm{K}-39}\right)$, the analytical description of the saturated water vapor pressure.

From this, the fit formula results:

$$\lambda = \lambda_{\mathrm{evac}}(T) + c' X_{\mathrm{w}}(\varphi) + d \frac{\lambda_{\mathrm{gas},0}}{p_{1/2}} p_{\mathrm{H_2O}}(T). \tag{8}$$

With the values given above and the use of a linear adsorption isotherm, one gets

$$\lambda = (a + bT) + c\varphi + d \frac{25.5}{600} p_{\mathrm{H_2O}}(T)\,. \tag{9}$$

A four-parameter fit for a, b, c, and d with measured λ, φ, and T yields satisfying agreement between measured and calculated data for all parameters varied. The resulting fit parameters are

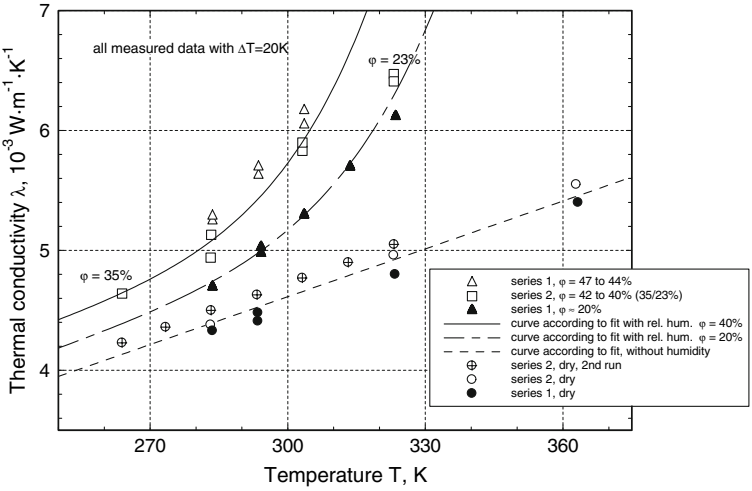

Fig. 10 Measured thermal conductivity for different water content and temperature. Additionally from the four-parameter-fit, the calculated thermal conductivity of the evacuated specimen is depicted, as well as for specimens with 20% and 40% relative humidity

$a = 0.624 \times 10^{-3}\mathrm{W \cdot m^{-1} \cdot K^{-1}}$, $b = 0.0133/K\,10^{-3}\ \mathrm{W \cdot m^{-1} \cdot K^{-1}}$, $c = 1.14 \times 10^{-3}\ \mathrm{W \cdot m^{-1} \cdot K^{-1}}$, and $d = 1.08$.

In Fig. 10 measured and calculated thermal conductivities are plotted as a function of temperature with the humidity as a parameter.

In the experiments it is difficult to maintain constant relative humidity upon temperature variation, because of partial condensation of water vapor at cold spots outside the specimens. In the first series of measurements, for a relatively high amount of water in the apparatus, the relative humidity varied from 47% to 44% when increasing the temperature from 284 to 304 K. Within the second series of measurements, for a slightly less amount of water in the apparatus, for the same temperature range, the relative humidity varied from 42% to 40%. At the even more extreme conditions, the relative humidity was reduced to 35% at 264 K and 23% at 323 K. For the smaller amount of water in the apparatus, in the first series, in the temperature range from 284 to 314 K the relative humidity was almost constant, $(20 \pm 1)\%$; only at 324 K it was reduced to 16%.

In Fig. 10 beside the experimental data with non-uniform relative humidity, calculated curves are also plotted according to the fit results. The calculated curves for 20% and 40% relative humidity coincide quite well with the measured thermal conductivity for similar water content levels.

From the fit parameter c, an effect of adsorbed water on the thermal conductivity of about $0.01 \times 10^{-3}\mathrm{W \cdot m^{-1} \cdot K^{-1}}$ per % of relative humidity is observed. A result for the fit parameter d of about 1 indicates that the onset of gaseous contributions to the total thermal conductivity is quite similar for water and for nitrogen.

It has to be pointed out that in the course of the different series of measurements with different moisturization and drying cycles, the thickness of the samples shrank from 18.6 to 18.2 mm. At the same time the thermal conductivity of the evacuated

specimen increased by about $0.4 \times 10^{-3} \mathrm{W \cdot m^{-1} \cdot K^{-1}}$, as may be seen from the three lowest curves in Fig. 10. It has to be checked whether possibly capillary forces at high humidity may be the reason.

4 Conclusion

The thermal conductivity of an 'evacuated' fumed silica board has been measured as a function of moisture content and temperature. Neglecting possible effects of mass transfer by vapor diffusion and counter surface and capillary diffusion, a simple model describes the influence of the moisture on the total thermal conductivity as an increase in the solid conductivity proportional to the amount of the adsorbed water and an effect of the vapor that is quite close to that of nitrogen gas. In the low-pressure region, typical for practical applications of VIPs, the increase caused by the water vapor again is proportional to the partial pressure.

Based on the adsorption isotherm, numerical calculations describe the moisture distribution in a VIP for a broad range of water content, temperatures, and temperature gradients. Parameter studies indicate that in the measurement practice, a dependence of the heat transfer coefficient on the temperature gradient is to be expected.

A more detailed analysis of the data, also with different temperature gradients, should give more insight into the moisture distribution and its effect on the total (apparent) thermal conductivity.

Up to now, the question of whether heat-pipe effects also have a significant impact on the total heat transfer could not be answered.

References

1. U. Heinemann, R. Caps, J. Fricke, Vuoto scienza et tecnologia **28**, 43 (1999)
2. R. Caps, U. Heinemann, M. Ehrmanntraut, J. Fricke, High Temp. High Press. **33**, 151 (2001)
3. H. Schwab, U. Heinemann, A. Beck, H.-P. Ebert, J. Fricke, Thermal Env. Bldg. Sci. **28**, 293 (2005)
4. U. Heinemann, J. Hetfleisch, R. Caps, J. Kuhn, J. Fricke, in *Advances in Thermal Insulations, Eurotherm Seminar No. 44, Espinho—Portugal*, ed. by ECEMEI (1995), pp. 155–164
5. J. Fricke, High Temp. High Press. **25**, 379 (1993)
6. U. Heinemann, R. Caps, J. Fricke, Int. J. Heat Mass Transfer **39**, 2115 (1996)
7. R. Caps, U. Heinemann, J. Fricke, K. Keller, Int. J. Heat Mass Transfer **40**, 269 (1997)
8. M.G. Kaganer, *Thermal Insulations in Cryogenic Engineering* (Program for Scientific Translations, IPST Press, Jerusalem, 1969)
9. S. Rudtsch, High Temp. High Press. **32**, 487 (2000)
10. C. Langlais, M. Hyrien, S. Klarsfeld, in *ASTM STP 789*, ed. by F.A. Govan, D.M. Greason, J.D. McAllister (1983), pp. 563–581
11. H. Schwab, U. Heinemann, A. Beck, H.-P. Ebert, J. Fricke, Thermal Env. Bldg. Sci. **28**, 319 (2005)